

Generation of the Probabilistic Template of Default Mode Network Derived from Resting-State fMRI

Journal:	<i>Transactions on Biomedical Engineering</i>
Manuscript ID:	TBME-01499-2013.R1
Manuscript Type:	Paper
Date Submitted by the Author:	n/a
Complete List of Authors:	<p>Wang, Defeng; The Chinese University of Hong Kong, Department of Imaging and Interventional Radiology Kong, Youyong; The Chinese University of Hong Kong, Department of Imaging and Interventional Radiology Chu, Winnie CW; The Chinese University of Hong Kong, Department of Imaging and Interventional Radiology Tam, Cindy; North District Hospital, Sheung Shui, Department of Psychiatry Lam, Linda; The Chinese University of Hong Kong, Department of Psychiatry Yilong, Wang; Beijing Tiantan Hospital, Capital Medical University, Department of Neurology Northoff, Georg; Institute of Mental Health Research, University of Ottawa, Mind, Brain Imaging and Neuroethics Mok, Vincent; The Chinese University of Hong Kong, Department of Medicine and Therapeutics Wang, Yongjun; Beijing Tiantan Hospital, Capital Medical University, Department of Neurology Shi, Lin; The Chinese University of Hong Kong, Department of Medicine and Therapeutics</p>
TIPS:	neuroimaging, resting-state fMRI, Default mode network, template, brain

1
2
3
4
5
6
7
8
9
10
11
12
13
14
15
16
17
18
19
20
21
22
23
24
25
26
27
28
29
30
31
32
33
34
35
36
37
38
39
40
41
42
43
44
45
46
47
48
49
50
51
52
53
54
55
56
57
58
59
60

Generation of the Probabilistic Template of Default Mode Network Derived from Resting-State fMRI

Defeng Wang^{1,2,3}, Youyong Kong^{1,2}, Winnie CW Chu^{1,2,*}, Cindy WC Tam⁴, Linda
CW Lam⁵, Yilong Wang⁶, Georg Northoff⁷, Vincent CT Mok^{8,9}, Yongjun Wang⁶, Lin
Shi^{8,9,**}

¹Department of Imaging and Interventional Radiology, The Chinese University of
Hong Kong, Shatin, NT, Hong Kong SAR, China

²Research Center for Medical Image Computing, The Chinese University of Hong
Kong, Shatin, NT, Hong Kong SAR, China

³CUHK Shenzhen Research Institute, Shenzhen, China

⁴Department of Psychiatry, North District Hospital, Sheung Shui, NT, Hong Kong

⁵Department of Psychiatry, The Chinese University of Hong Kong, Shatin, NT, Hong
Kong SAR, China

⁶Department of Neurology, Beijing Tiantan Hospital, Capital Medical University,
Beijing, PR China

⁷Mind, Brain Imaging and Neuroethics, Institute of Mental Health Research,
University of Ottawa, Ottawa, ON, Canada

⁸Department of Medicine and Therapeutics, The Chinese University of Hong Kong,
Shatin, Hong Kong SAR, China

⁹Lui Che Woo Institute of Innovation Medicine, The Chinese University of Hong
Kong, Shatin, Hong Kong SAR, China

1
2
3
4 **Corresponding Author:**
5

6 * Winnie CW Chu (for clinical issues); Email address: winnie@med.cuhk.edu.hk
7

8
9 ** Lin Shi (for technical issues); Email address: shilin@cuhk.edu.hk
10

11
12 **Mailing address:** Department of Imaging and Interventional Radiology, The Chinese
13

14 University of Hong Kong, Shatin, New Territories, Hong Kong.
15
16
17
18
19
20
21
22
23
24
25
26
27
28
29
30
31
32
33
34
35
36
37
38
39
40
41
42
43
44
45
46
47
48
49
50
51
52
53
54
55
56
57
58
59
60

For Review Only

Generation of the Probabilistic Template of Default Mode Network Derived from Resting-State fMRI

Abstract

Default-mode network (DMN) has become a prominent network among all large-scale brain networks which can be derived from the resting-state fMRI (rs-fMRI) data. Statistical template labelling the common location of hubs in DMN is favourable in the identification of DMN from tens of components resulted from the independent component analysis (ICA). This paper proposed a novel iterative framework to generate a probabilistic DMN template from a coherent group of 40 healthy subjects. An initial template was visually selected from the independent components derived from group ICA analysis of the concatenated rs-fMRI data of all subjects. An effective similarity measure was designed to choose the best-fit component from all independent components of each subject computed given different component numbers. The selected DMN components for all subjects were averaged to generate an updated DMN template and then used to select the DMN for each subject in the next iteration. This process iterated until the convergence was reached, i.e., overlapping region between the DMN areas of current template and the one generated from the previous stage is more than 95%. By validating the constructed DMN template on the rs-fMRI data from another 40 subjects, the generated probabilistic DMN template and the proposed similarity matching mechanism were demonstrated to be effective in automatic selection of independent components from the ICA analysis results.

Key words: Default mode network, resting-state fMRI, template, brain network.

Introduction

Over the last few decades, there has been growing interest in investigating the large-scale brain networks that exist in the human cognition, perception and emotion. The default-mode network (DMN) is a prominent one among these discovered brain networks. The commonly accepted hubs of DMN include the posterior cingulate cortex (PCC), the medial temporal lobes (MTL), the medial prefrontal cortex (mPFC) and the angular gyrus (AG) [1, 2]. These related brain regions are considered to be active during resting state while deactivated when specific purposeful cognitive tasks are performed. Moreover, the DMN has been suggested to be related to various cognitive functions and be altered in a series of neuropsychological disorders [3, 4].

The identification of DMN has been extensively studied in both healthy individuals and subjects of various pathological conditions from resting state fMRI (rsfMRI) [5]. Plenty of methods have been proposed to derive the DMN from the rsfMRI datasets [6-8]. Among these approaches, the method using independent component analysis (ICA) has been widely utilized to extract networks in previous studies [9, 10]. ICA technique enables the blind-source separation of mixed signals into independent spatial and temporal components, which are considered to represent different functionally connected networks [6, 11]. However, there remains the problem of how to accurately select the component that best represents the DMN from the numerous components. Manual selection may be time consuming as all components should be carefully visualized and analysed. One objective approach is to automatically select the best-fit component by matching with a given DMN template [12, 13].

1
2
3
4 Therefore, a standardized DMN template representing the statistical location of the hubs is
5
6 demanding for objective component selections.
7
8

9
10 Plenty of approaches have been so far proposed to construct the statistical structural brain
11
12 template. In the early 1990s, Evans, et al. [14] introduced the concept of a statistical MRI
13
14 template for brain mapping. They constructed the MNI305 template by linearly mapping 305
15
16 native MRI volumes to a manually-derived average MRI. In 1998, Holmes, et al. [15] created
17
18 a new atlas with much higher signal-to-noise ratio. One subject was scanned 27 times, and all
19
20 the images were linearly registered to compute an average which was finally mapped to
21
22 MNI305. However, linear registration can't capture the local deformation between different
23
24 subjects. In 2000, Guimond, et al. [16] developed a method of building a template atlas by
25
26 nonlinearly registered each subject to an initial template. With all nonlinear transformations,
27
28 original images were resampled to construct a template with an average unbiased shape and
29
30 average intensity. Recently, Fonov, et al. [17] proposed an iterative approach to create an
31
32 unbiased non-linear statistical atlas that were not subject to the vagaries of any single brain.
33
34 This procedure consisted of 40 iterations, and at each iteration native volumes were
35
36 non-linearly fitted to the template from the previous iteration. Being different from
37
38 constructing statistical brain template derived directly from scanned MRI volumes, DMN
39
40 template cannot be directly computed from fMRI data. Therefore, the proposed structural
41
42 brain atlas generation algorithms could not be directly extended to the construction of DMN
43
44 template.
45
46
47
48
49
50
51
52
53
54
55
56
57
58
59
60

1
2
3
4 To construct a DMN template, researchers have proposed a lot of approaches, which can be
5
6 classified into two groups. One strategy is to manually select some regions from a structural
7
8 brain atlas to generate a template [18, 19]. However, there exist some inconsistencies in
9
10 determining the neuronal regions to compose a DMN template. The other approach is to
11
12 perform a group-level ICA analysis to produce a “distributed” template [20, 21]. In this way,
13
14 the fMRI data from all the subjects is first concatenated to form one 4D dataset. The DMN
15
16 template is then visually recognized from the independent components that are produced by
17
18 the ICA analysis on the concatenated 4D dataset. However, the difference among the fMRI
19
20 data of each subject may not capture the intrinsic functional connectivity [22]. The
21
22 concatenated data can’t well reflect the temporal relationship in the fMRI data of each subject,
23
24 and thus the resulting template may not fully preserve the information in the original data.
25
26 Moreover, only a few subjects were utilized to generate the template [23]. Therefore, it is of
27
28 great importance to construct a statistically representative template for DMN.
29
30
31
32
33
34
35
36

37 This paper presents a novel framework to generate a probabilistic DMN template from
38
39 resting-state fMRI. Inspired by the structural brain atlas generation, an iterative approach was
40
41 developed to create an unbiased DMN template. Resting-state fMRI data from 50 healthy
42
43 subjects were utilized to generate the template. An initial template was visually selected from
44
45 the independent components, which were obtained by performing ICA analysis on the
46
47 concatenated fMRI data from all the 50 subjects using FSL melodic software. For each
48
49 subject, as the selection of component number could affect the ability to capture the
50
51 resting-state functional connectivity, independent components were obtained on different
52
53
54
55
56
57
58
59
60

1
2
3
4 component numbers. To find the DMN from the components in each subject, we developed a
5
6 specific similarity measure. The component with the highest similarity was selected as the
7
8 DMN component for each subject. All the selected DMN components were then averaged to
9
10 generate a refined DMN template. The iteration process would stop once overlapping region
11
12 between the DMN areas of current template and the one generated from the previous stage
13
14 was more than 95%. All selected components were finally masked with a given z score. By
15
16 averaging all the masks, a statistical DMN template was achieved. Resting-state data from
17
18 another forty subjects were utilized to validate the automatic component selection method
19
20 using the constructed statistical template.
21
22
23
24

25 26 27 **Materials and Methods**

28 29 30 *Subjects and Image Acquisition*

31
32
33 Ninety healthy subjects (age range, 60 – 89; mean age, 73; 48 females; all right-handed) were
34
35 scanned at the resting-state. The resting state fMRI series were acquire on a 3T Philips
36
37 Medical Systems (Achieva, Philips, Germany), using the 8-channel head coil. Subjects were
38
39 instructed to relax and keep their eyes open. In each scanning sequence, we obtained a series
40
41 of 40 axial T2-weighted gradient echo-planar images (repetition time (TR) = 3000ms, echo
42
43 time (TE) = 25ms, flip angle = 90°, field of view (FOV) = 220×220mm², matrix = 64×64,
44
45 in-plane resolution=2.4×2.4mm², slice thickness=3mm). Eighty volumes were acquired in the
46
47 resting-state functional scan for each subject. Three-dimensional T1-weighted images (TR =
48
49 18 ms, TE= 2ms, flip angle= 30°, voxel size = 1.04×1.04×0.6 mm³) were acquired in the same
50
51
52
53
54
55
56
57
58
59
60

1
2
3
4 session in order to have high-resolution spatial references for registration and normalization
5
6 of the functional images.
7

8 9 ***Pre-processing of rs-fMRI data***

10
11
12 Among the 90 subjects, 50 subjects were used to generate the template and the other 40
13
14 subjects were used for evaluation. Functional MRI data of all the 90 subjects was
15
16 preprocessed using SPM8 (www.fol.ion.ucl.ac.uk/spm). Time series images were first
17
18 spatially registered to the MNI space using spatial normalisation. This could minimize the
19
20 misalignment due to patient motion and correct for slice-time acquisition differences. Images
21
22 were then resampled into $2 \times 2 \times 2$ mm³ and spatially blurred using an 8-mm Gaussian
23
24 full-width half-maximum filter.
25
26
27
28
29

30 31 ***Generation of Anatomical Brain Template***

32
33
34 The anatomical T1W images of the 50 healthy subjects were nonlinearly registered and
35
36 transformed to the T1W template using spatial normalization tool provided by SPM8. All the
37
38 transformed images were finally averaged and spatially blurred using a 6-mm Gaussian
39
40 full-width half-maximum filter to generate an anatomical brain template.
41
42
43
44

45 46 ***Generation of the Initial Template***

47
48
49 Resting-state fMRI data from fifty healthy subjects was utilized to construct the template. To
50
51 construct a template, an initial template should be first given to guide the template generation
52
53 process. In structural MRI, the initial template was always a single volume of one subject or
54
55 an average of native MRI volumes. However, the initial template couldn't be directly
56
57
58
59
60

1
2
3
4 obtained from the fMRI data. An appropriate way to obtain an initial template was to perform
5
6 a group-level ICA analysis.
7

8
9
10 For each subject, the smoothed normalized fMRI images were concatenated across time to
11
12 form a single 4D volumetric dataset. All the preprocessed images from each subject were then
13
14 concatenated into one set of 4D image. The 4D images with all the subjects were then
15
16 processed with FSL melodic ICA software (<http://www.fmrib.ox.ac.uk/fsl/index.html>). The
17
18 Melodic software utilized probabilistic ICA to estimate the number of relevant noise and
19
20 signal sources in the 4D data. The number of components was automatically estimated.
21
22 Afterwards, the fMRI data was decomposed into a set of spatially independent maps. These
23
24 maps provided intensity values (z scores) and thus a measure of the contribution of the time
25
26 course of a component to the signal for a given voxel. The initial DMN template was finally
27
28 selected visually based on their correspondence to the DMN identified by Damoiseaux, et al.
29
30 [24]. Fig.1 shows the selected initial DMN template from the estimated maps.
31
32
33
34
35
36
37

38 *Similarity Measure between DMN Components*

39

40
41 For each subject, ICA analysis was also carried out using FSL Melodic software. For each
42
43 subject, there were a large number of spatial maps. It was time consuming to select the
44
45 best-fit component by visually comparing among all the components. To automatically select
46
47 the most similar component, we developed an effective similarity measurement algorithm. Z
48
49 scores reflect the degree to which a given voxel's time series was correlated with the time
50
51 series corresponding to the specific ICA component. Similarity between the independent
52
53
54
55
56
57
58
59
60

components and the template was defined as the absolute value between their z maps derived from the melodic as equation (1),

$$s(z_i, z_t) = \left| \frac{1}{M} \sum_{m=1}^M \left[\left(\frac{z_i(m) - \bar{z}_i}{\delta_{z_i}} \right) \left(\frac{z_t(m) - \bar{z}_t}{\delta_{z_t}} \right) \right] \right|, \quad (1)$$

where z_i and z_t are the z-value of M voxels in the common mask of the z-value maps of the i-th component and the initial template, \bar{z}_i and \bar{z}_t are the mean values of the z_i and z_t , δ_{z_i} and δ_{z_t} are the corresponding standard deviations.

Iterative Procedure for Template Refinement

The selection of the number of components (N) could influence the ability of spatial component to capture the resting state functional connectivity [25]. Setting N too small could squeeze independent networks to the same component. On the other hand, hubs belonging to the same network might be separated into different components if N was set too big. Although some researchers estimated the appropriate number of ICA components for fMRI data, it could vary across different individuals [26]. Therefore, in order to obtain real independent components, multiple types of component numbers were utilized in our approach, i.e., 10, 15, 20, 25, 30, 35, 40, 50, 60 and 70. Best-fit components were selected by matching with the initial DMN template using the proposed similarity measure.

The main procedure of the template generation algorithm is illustrated as Fig. 2. Starting with the initial template, we iteratively selected the best-fit component from the independent components of each subject and reconstructed a refined DMN template. For each subject,

1
2
3
4 similarity between each component with the current DMN template was computed. Only the
5
6 component with the highest similarity was selected as the DMN component for that subject.
7
8
9 All the selected components were then averaged to generate a refined DMN template. The
10
11 DMN template was then thresholded with a given z score to extract the DMN area. The
12
13 termination criterion was that the similarity measurement between the DMN areas of current
14
15 template and the one generated from the previous stage was more than 95%. Fig. 5 illustrates
16
17 the similarities between templates generated from adjacent stages during the iterations. The
18
19 procedure stopped after six iterations in our experiment. All selected components were finally
20
21 thresholded with a given z score. By averaging all the masks, a statistical DMN template was
22
23 achieved. The template was further smoothed using a 6-mm Gaussian full-width
24
25 half-maximum filter.
26
27
28
29
30
31

32 **Results**

33 *Templates*

34
35
36
37
38 The sagittal, coronal, and axial views of the anatomical template are shown in Fig. 3. Fig. 4
39
40 shows the statistical DMN template derived from the 50 healthy subjects. The DMN template,
41
42 a sample dataset, the DMN selected using the proposed method, and the Matlab code of DMN
43
44 selection and similarity measurement are downloadable at
45
46
47 http://www.droid.cuhk.edu.hk/staff/staff_list/dfwang/dmn.htm. The identified areas were
48
49
50 consistent with binary DMN templates generated in previous works [1, 3, 25].
51
52
53
54

55 *Validation of the Statistical Template*

To validate the automatic component selection method using the statistical template, we employed here the resting-state fMRI data from the rest 40 subjects. ICA analysis was performed on the resting-state data for each subject using Melodic software. Independent components were also generated in a range of components numbers: 10, 15, 20, 25, 30, 35, 40, 50, 60 and 70. We first applied the proposed automatic selection approach to choose the best-fit DMN components among numerous components. On the other hand, we visually selected DMN components from the acquired components. The DMN components from automatic and manual selections were all thresholded to achieve the DMN. To evaluate the automatic selection result, the Dice coefficient was used to measure the spatial overlap between the two DMN maps for each subject. With the binary DMN z_a and z_v from the automatic and visual selection, the dice coefficient was defined as

$$d(z_a, z_v) = \frac{2|z_a \cap z_v|}{|z_a| + |z_v|}. \quad (2)$$

Dice coefficients have a restricted range of [0,1], where 0 represents that there is no overlap and 1 denotes that they are perfectly overlapped. Fig. 6 gives the Dice coefficients for all the 40 subjects. Most of the values were equal to 1 and all the other ones were very close to 1. This indicated that the DMN selected with the automatic method was quite similar to the visually selected results.

We further evaluate the superiority of our statistical template by comparing with the traditional binary template. The binary template was obtained by thresholding the recognized DMN component from group-ICA analysis. This was widely used in previous studies [20, 21].

1
2
3
4 We computed the dice coefficients of the manually selected DMN of each subject with the
5
6 two templates. Fig. 7 gives the dice coefficients of the DMN of each subject on the two
7
8 templates. The statistical template obtained higher dice coefficient than initial binary template.
9
10
11 This demonstrated that the statistical template was more consistent with the DMN
12
13 distribution.
14

15 16 17 **Discussion**

18
19
20 We presented a novel iterative method for creating a statistical DMN template through
21
22 resting-state fMRI data from a large number of subjects. Our method used iterative
23
24 refinement with an effective similarity measurement algorithm to select the DMN component
25
26 from the numerous independent components for each subject. The iteration process
27
28 terminated until the difference between the templates of the current and previous stage was
29
30 less than 5%. With all the masks of the DMN areas from each subject being averaged, the
31
32 statistical DMN template was achieved. For validation, unseen data from another forty
33
34 healthy subjects were employed. The results demonstrated that the DMN can be accurately
35
36 selected with the currently constructed statistical template.
37
38
39
40
41
42

43
44 Our template-building algorithm is different from the iterative methods for brain structural
45
46 template in the following ways. In the construction of traditional structural MRI template,
47
48 data was directly used to generate the template. Here, the template was constructed from the
49
50 independent components which were derived from ICA analysis on resting-state fMRI data.
51
52 The initial template was visually selected from the independent components that derived from
53
54 group ICA analysis on the concatenated data of all subjects. This is quite different from
55
56
57
58
59
60

1
2
3
4 traditional structural MRI that takes a single subject data or the averaged data as an initial
5
6 template. Previous methods performed ICA analyses on a specific or an automatically
7
8 estimated component number. This differs from our method that utilized multiple types of
9
10 component numbers to better capture the resting-state functional connectivity.
11
12

13
14 Previous DMN templates were often derived from group-level ICA analysis with binary
15
16 masks. All fMRI data from all the subjects was concatenated to form one 4D dataset. DMN
17
18 templates were visually recognized among the components from ICA analysis on the 4D
19
20 dataset. The templates are binary masks from a few subjects [20, 21, 23]. In our approach, a
21
22 large number of healthy subjects were employed to generate the probabilistic template.
23
24 Compared with the binary templates, probabilistic template could better represent the
25
26 statistical DMN distribution within a population. Limited by the data at hand, present
27
28 template was constructed from the older subjects only. The connectivity in DMN has been
29
30 demonstrated to be changed with normal aging [27]. The DMN template may have
31
32 differences for different age stages. In future, more subjects with a wider age range will be
33
34 employed to refine the statistical template and construct new age-specific templates. The
35
36 algorithm can also be extended to create template for other types of brain networks, such as
37
38 the executive control network, the salience network, and the sensorimotor network, etc.
39
40
41
42
43
44
45
46

47
48 The probabilistic DMN template and the implementation of the similarity measurement will
49
50 be available online for free download. The proposed DMN template can serve as an unbiased
51
52 reference for the identification of DMN from resting-state fMRI, and hopefully can be
53
54 adopted as a useful tool for further research into the brain network.
55
56
57

60

Acknowledgement

The work described in this paper was supported by grants from the Research Grants Council of the Hong Kong Special Administrative Region, China (Project No.: CUHK 475711, 411910, 411811), a grant from the Science, Industry, Trade and Information Commission of Shenzhen Municipality (Project No. JC201005250030A), and a grant from the National Natural Science Foundation of China (Project No. 81101111).

Figure Legend

Fig. 1. Initial DMN template

Fig. 2. Flowchart of the DMN generation process

Fig. 3. Anatomical template

Fig. 4. DMN statistical template mapped onto the anatomical template

Fig. 5. Similarities between templates of adjacent stage during the iterations

Fig. 6. Dice coefficients between automatic and manual DMN selection

Fig. 7. Comparison of dice coefficients of the manually selected DMN with the statistical template and the initial binary template

Reference

- 1
2
3 [1] K. Supekar, L. Q. Uddin, K. Prater, H. Amin, M. D. Greicius, and V. Menon,
4 "Development of functional and structural connectivity within the default mode
5 network in young children," *Neuroimage*, vol. 52, pp. 290-301, Aug 1 2010.
- 6 [2] F. De Vogelaere, P. Santens, E. Achten, P. Boon, and G. Vingerhoets, "Altered
7 default-mode network activation in mild cognitive impairment compared with healthy
8 aging," *Neuroradiology*, Apr 12 2012.
- 9 [3] M. D. Greicius, G. Srivastava, A. L. Reiss, and V. Menon, "Default-mode network
10 activity distinguishes Alzheimer's disease from healthy aging: evidence from
11 functional MRI," *Proc Natl Acad Sci U S A*, vol. 101, pp. 4637-42, Mar 30 2004.
- 12 [4] G. Mingoia, G. Wagner, K. Langbein, R. Maitra, S. Smesny, M. Dietzek, *et al.*,
13 "Default mode network activity in schizophrenia studied at resting state using
14 probabilistic ICA," *Schizophr Res*, vol. 138, pp. 143-9, Jul 2012.
- 15 [5] E. Widjaja, M. Zamyadi, C. Raybaud, O. C. Snead, and M. L. Smith, "Impaired
16 Default Mode Network on Resting-State fMRI in Children with Medically Refractory
17 Epilepsy," *American Journal of Neuroradiology*, vol. 34, pp. 552-557, Mar 2013.
- 18 [6] C. F. Beckmann and S. A. Smith, "Probabilistic independent component analysis for
19 functional magnetic resonance imaging," *Ieee Transactions on Medical Imaging*, vol.
20 23, pp. 137-152, Feb 2004.
- 21 [7] M. H. Lee, C. D. Hacker, A. Z. Snyder, M. Corbetta, D. Y. Zhang, E. C. Leuthardt, *et*
22 *al.*, "Clustering of Resting State Networks," *Plos One*, vol. 7, Jul 9 2012.
- 23 [8] R. F. Qi, L. J. Zhang, Q. Xu, J. H. Zhong, S. Y. Wu, Z. Q. Zhang, *et al.*, "Selective
24 Impairments of Resting-State Networks in Minimal Hepatic Encephalopathy," *Plos*
25 *One*, vol. 7, May 25 2012.
- 26 [9] C. Rosazza, L. Minati, F. Ghielmetti, M. L. Mandelli, and M. G. Bruzzone,
27 "Functional Connectivity during Resting-State Functional MR Imaging: Study of the
28 Correspondence between Independent Component Analysis and
29 Region-of-Interest-Based Methods," *American Journal of Neuroradiology*, vol. 33,
30 pp. 180-187, Jan 2012.
- 31 [10] G. V. Pendse, D. Borsook, and L. Becerra, "A Simple and Objective Method for
32 Reproducible Resting State Network (RSN) Detection in fMRI," *Plos One*, vol. 6,
33 Dec 12 2011.
- 34 [11] Y. Deng, Q. H. Dai, and Z. K. Zhang, "Graph Laplace for Occluded Face Completion
35 and Recognition," *Ieee Transactions on Image Processing*, vol. 20, pp. 2329-2338,
36 Aug 2011.
- 37 [12] A. R. Franco, A. Pritchard, V. D. Calhoun, and A. R. Mayer, "Interrater and
38 intermethod reliability of default mode network selection," *Hum Brain Mapp*, vol. 30,
39 pp. 2293-303, Jul 2009.
- 40 [13] P. G. Samann, R. Wehrle, D. Hoehn, V. I. Spoormaker, H. Peters, C. Tully, *et al.*,
41 "Development of the Brain's Default Mode Network from Wakefulness to Slow
42 Wave Sleep," *Cerebral Cortex*, vol. 21, pp. 2082-2093, Sep 2011.
- 43 [14] A. C. Evans, S. Marrett, P. Neelin, L. Collins, K. Worsley, W. Dai, *et al.*,
44 "Anatomical mapping of functional activation in stereotactic coordinate space,"
45 *Neuroimage*, vol. 1, pp. 43-53, Aug 1992.

- 1
2
3 [15] C. J. Holmes, R. Hoge, L. Collins, R. Woods, A. W. Toga, and A. C. Evans,
4 "Enhancement of MR images using registration for signal averaging," *Journal of*
5 *Computer Assisted Tomography*, vol. 22, pp. 324-333, Mar-Apr 1998.
6
7 [16] A. Guimond, J. Meunier, and J. P. Thirion, "Average brain models: A convergence
8 study," *Computer Vision and Image Understanding*, vol. 77, pp. 192-210, Feb 2000.
9
10 [17] V. Fonov, A. C. Evans, K. Botteron, C. R. Almli, R. C. McKinstry, and D. L. Collins,
11 "Unbiased average age-appropriate atlases for pediatric studies," *Neuroimage*, vol. 54,
12 pp. 313-27, Jan 1 2011.
13
14 [18] R. P. Dhond, C. Yeh, K. Park, N. Kettner, and V. Napadow, "Acupuncture modulates
15 resting state connectivity in default and sensorimotor brain networks," *Pain*, vol. 136,
16 pp. 407-18, Jun 2008.
17
18 [19] V. Napadow, L. LaCount, K. Park, S. As-Sanie, D. J. Clauw, and R. E. Harris,
19 "Intrinsic Brain Connectivity in Fibromyalgia Is Associated With Chronic Pain
20 Intensity," *Arthritis and Rheumatism*, vol. 62, pp. 2545-2555, Aug 2010.
21
22 [20] F. Esposito, A. Aragri, I. Pesaresi, S. Cirillo, G. Tedeschi, E. Marciano, *et al.*,
23 "Independent component model of the default-mode brain function: combining
24 individual-level and population-level analyses in resting-state fMRI," *Magn Reson*
25 *Imaging*, vol. 26, pp. 905-13, Sep 2008.
26
27 [21] C. C. Guo, F. Kurth, J. Zhou, E. A. Mayer, S. B. Eickhoff, J. H. Kramer, *et al.*,
28 "One-year test-retest reliability of intrinsic connectivity network fMRI in older
29 adults," *Neuroimage*, vol. 61, pp. 1471-83, Jul 16 2012.
30
31 [22] Y. Deng, Y. Y. Zhao, Y. B. Liu, and Q. H. Dai, "Differences Help Recognition: A
32 Probabilistic Interpretation," *Plos One*, vol. 8, Jun 3 2013.
33
34 [23] C. Habas, N. Kamdar, D. Nguyen, K. Prater, C. F. Beckmann, V. Menon, *et al.*,
35 "Distinct cerebellar contributions to intrinsic connectivity networks," *J Neurosci*, vol.
36 29, pp. 8586-94, Jul 1 2009.
37
38 [24] J. S. Damoiseaux, S. A. Rombouts, F. Barkhof, P. Scheltens, C. J. Stam, S. M. Smith,
39 *et al.*, "Consistent resting-state networks across healthy subjects," *Proc Natl Acad Sci*
40 *U S A*, vol. 103, pp. 13848-53, Sep 12 2006.
41
42 [25] A. Abou-Elseoud, T. Starck, J. Remes, J. Nikkinen, O. Tervonen, and V. Kiviniemi,
43 "The effect of model order selection in group PICA," *Hum Brain Mapp*, vol. 31, pp.
44 1207-16, Aug 2010.
45
46 [26] L. S. Ma, B. Q. Wang, X. Y. Chen, and J. H. Xiong, "Detecting functional
47 connectivity in the resting brain: a comparison between ICA and CCA," *Magn Reson*
48 *Imaging*, vol. 25, pp. 47-56, Jan 2007.
49
50 [27] L. Geerligts, N. M. Maurits, R. J. Renken, and M. M. Lorist, "Reduced specificity of
51 functional connectivity in the aging brain during task performance," *Hum Brain*
52 *Mapp*, vol. 35, pp. 319-30, Jan 2014.
53
54
55
56
57
58
59
60

1
2
3 Dear Editor and Reviewers,
4

5 Thank you very much for your supportive and constructive comments. We have thoroughly
6 checked the manuscript and made the modifications accordingly to your suggestions.
7

8
9 Best regards,

10
11 Lin Shi
12

13
14
15 Reviewer's Comments
16

17
18
19 Reviewer: 1

20
21 Comments to the Author

22 The manuscript entitled Generation of the Probabilistic Template of Default Mode Network
23 Derived from Resting-State fMRI generated a probabilistic template for DMN using resting state
24 fMRI data. This work is interesting and useful to the brain imaging community.

25 I have several questions as follows:

26
27 1. The dataset used to generate the template only includes old people. Does age make a
28 difference to the template?
29

30 Reply: The connectivity in DMN has been demonstrated to be changed with normal aging [1].
31 The DMN template may have differences for different age stages. In our study, old subjects were
32 utilized to generate template. Our developed approach can be directly utilized generate templates
33 for available datasets from subjects with other age stages. The detailed description has been
34 added in the Discussion section (Page 14, Paragraph 2).
35
36

37 [1] Geerligns L, Maurits NM, Renken RJ, Lorist MM. Reduced specificity of functional
38 connectivity in the aging brain during task performance. Human Brain Mapping. 2014
39 35(1):319-30.
40
41

42
43 2. How sensitive is the template to the similarity metric and smoothing kernel size used in
44 the manuscript?
45

46 Reply: Different from traditional metric, the defined similarity metric measured the distance
47 between the z maps of the independent components. It was specifically designed to characterize
48 the difference of the distributions in two components. Few other similarity metrics have been
49 proposed for measuring the distance of z maps. Our defined metric was non-parametric. In the
50 metric definition, M means the number of voxels, z represents the mean value of z maps and δ is
51 the standard deviation of the z values in the z map.
52
53

54
55 3. I'm curious about how the iteration procedure converges. The authors used a hard
56 threshold (95% overlap with previous iteration), and it took 6 iterations to reach that requirement.
57
58
59
60

1
2
3 It would be helpful to have a table/figure to show how the overlap ratio changes along iteration
4 times. Also, when the iteration converges, does the z-score map of each subject represent DMN?
5
6

7 Reply: Thank you very much for the kind suggestions. Figure 5 has been added as suggested. As
8 the iteration converges, z-score map indicates the DMN for each subject.
9
10

11 4. I can't open the link to the website:

12 http://www.droid.cuhk.edu.hk/web/staff/staff_list/dfwang/dmn.htm
13
14

15 Reply: Many thanks for pointing out this problem. The correct link to the website is as follows.
16

17 http://www.droid.cuhk.edu.hk/staff/staff_list/dfwang/dmn.htm
18
19

20 We have updated the link in the manuscript.
21

22 5. Does it make sense to up-sample fMRI images to 2mm isotropic considering the original
23 ones are just 2.4mm*2.4mm*3mm?
24
25

26 Reply: In various studies, fMRI images are always registered to a same template for meaningful
27 comparisons. In general, fMRI images are up-sampled or down-sampled to align to a template
28 with similar spatial resolution [1,2].
29
30

31 [1] Di X, Biswal BB. Identifying the default mode network structure using dynamic causal
32 modeling on resting-state functional magnetic resonance imaging. *Neuroimage*. 2014;86:53-9.

33 [2] Cha J, Jo HJ, Kim HJ, Seo SW, Kim HS, Yoon U, Park H, Na DL, Lee JM. Functional
34 alteration patterns of default mode networks: comparisons of normal aging, amnesic mild
35 cognitive impairment and Alzheimer's disease. *Eur J Neurosci*. 2013;37(12):1916-24.
36
37
38
39

40 6. How to generate traditional binary DMN (P13, L30) should be more detailed.
41 Probabilistic template may cover more areas than its binary counterpart. Therefore, the
42 overlapping ratio by the probabilistic template might be theoretically larger than that by binary
43 template using the metric at P13.
44
45

46 Reply: We have added more detailed description of binary DMN generation as suggested (Page
47 12, paragraph 2). The overlapping ratio may not demonstrate the superiority of the statistical
48 template. We have changed to compute the dice coefficients to make a better demonstration.
49 Figure 7 provides the updated dice coefficients of selected DMN component from the statistical
50 template and binary template.
51
52
53
54
55
56
57
58
59
60

1
2
3 Reviewer: 2
4

5
6 Comments to the Author

7 This is a well written manuscript wherein the authors propose an automatic procedure for
8 identifying the DMN from ICA results. I have two minor comments which will improve the
9 manuscript:
10

11 1. A figure showing the convergence of the iteration is required. Plot iteration on x axis and
12 similarity index on y axis
13

14
15 Reply: Thanks for the king suggestion. We have added figure 5 as suggested.
16

17
18 2. The population as well as scan parameters are pretty atypical. The population itself represents
19 only older adults. TR= 3s is pretty long since newer scanners and sequences have made TRs
20 typically lesser than 2 s. Also, 80 volumes is pretty less for a resting state scan. The authors need
21 to comment on the effect of these atypical parameters
22

23
24 Reply: Thank you for the kind suggestion. In our study, only older subjects were included to
25 generate a probabilistic template. The dataset was utilized to evaluate the framework of default
26 mode network template generation. Our approach can also be utilized on datasets from other age
27 stages. The discussion was added to the Discussion section (Page 14, Paragraph 2).
28

29 For repetition time (TR), the values range from 2s to 3s in recent studies [1,2]. Two second is a
30 better choice. Thank you for the kind suggestions. We will change our imaging parameters for
31 scanning new subjects.
32

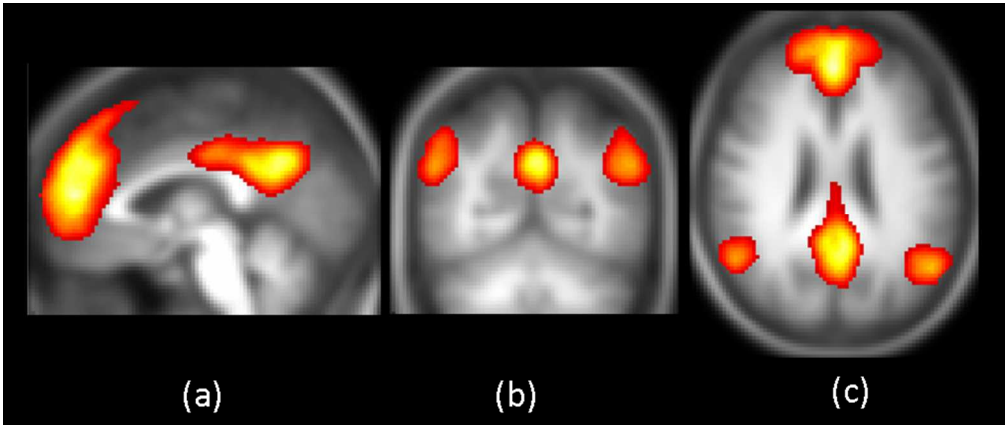
33
34 Eighty volumes are pretty less for a resting state scan. Our experimental results demonstrated
35 that the regions of obtained default mode networks were consistent with previous studies. This
36 may indicate that the acquired volumes were enough for independent component analysis. Some
37 previous studies also utilized 80 volumes rsfMRI for analysis, for instance [3].
38

39
40
41 [1] Geerligs L, Maurits NM, Renken RJ, Lorist MM. Reduced specificity of functional
42 connectivity in the aging brain during task performance. *Human Brain Mapping*. 2014
43 35(1):319-30.
44

45 [2] Cha J, Jo HJ, Kim HJ, Seo SW, Kim HS, Yoon U, Park H, Na DL, Lee JM. Functional
46 alteration patterns of default mode networks: comparisons of normal aging, amnesic mild
47 cognitive impairment and Alzheimer's disease. *Eur J Neurosci*. 2013 37(12):1916-24.
48

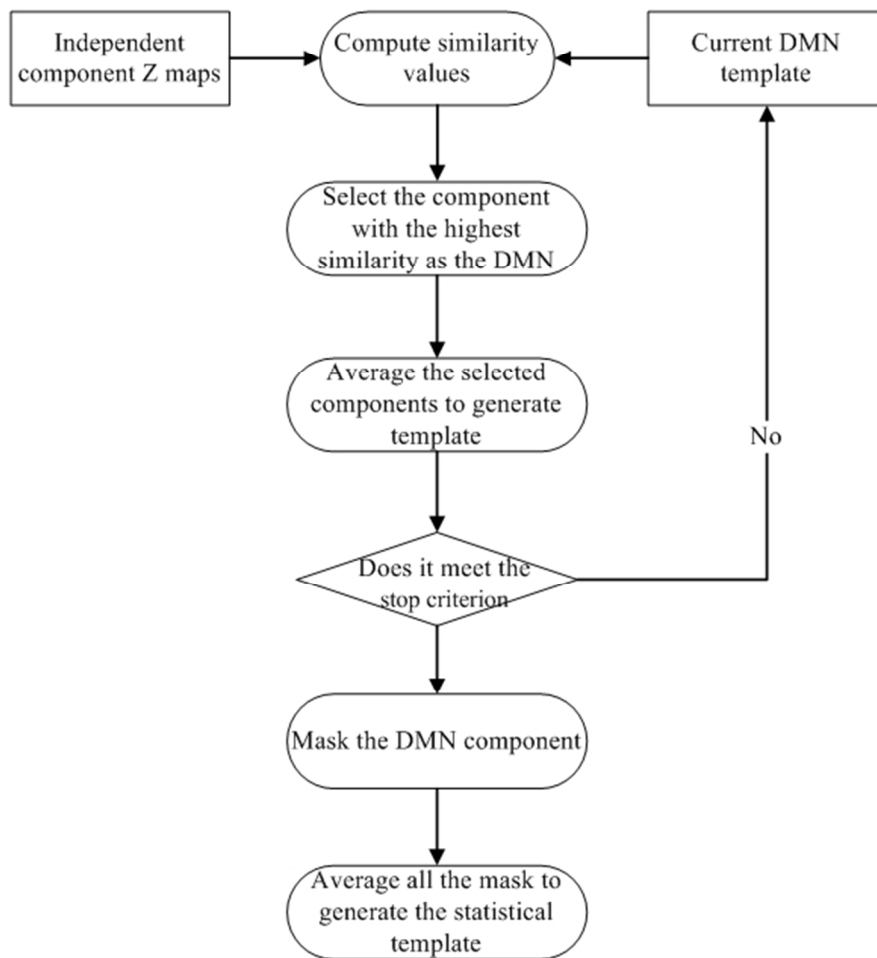
49 [3] Alonso-Solís A, Corripio I, de Castro-Manglano P, Duran-Sindreu S, Garcia-Garcia M, Proal
50 E, Nuñez-Marín F, Soutullo C, Alvarez E, Gómez-Ansón B, Kelly C, Castellanos FX. Altered
51 default network resting state functional connectivity in patients with a first episode of
52 psychosis. *Schizophr Research*. 2012 139(1-3):13-8.
53
54
55
56
57
58
59
60

1
2
3
4
5
6
7
8
9
10
11
12
13
14
15
16
17
18
19
20
21
22
23
24
25
26
27
28
29
30
31
32
33
34
35
36
37
38
39
40
41
42
43
44
45
46
47
48
49
50
51
52
53
54
55
56
57
58
59
60



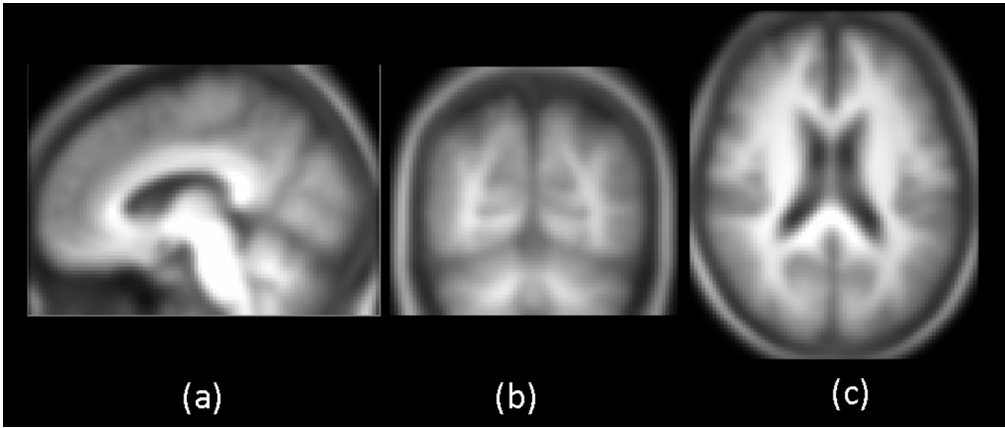
Initial DMN template
85x36mm (300 x 300 DPI)

Review Only



Flowchart of the DMN generation process
175x184mm (96 x 96 DPI)

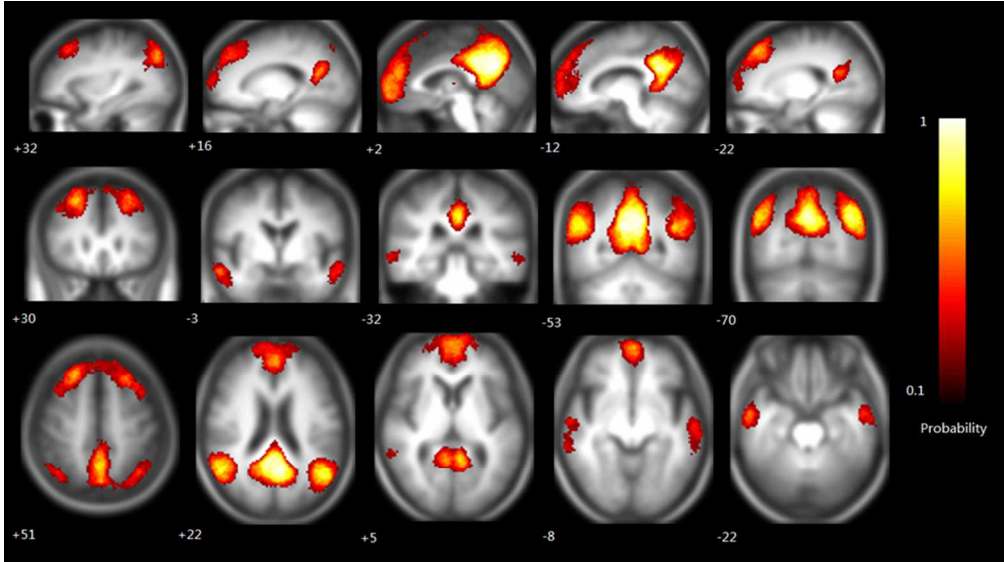
1
2
3
4
5
6
7
8
9
10
11
12
13
14
15
16
17
18
19
20
21
22
23
24
25
26
27
28
29
30
31
32
33
34
35
36
37
38
39
40
41
42
43
44
45
46
47
48
49
50
51
52
53
54
55
56
57
58
59
60



Anatomical template
85x36mm (300 x 300 DPI)

Review Only

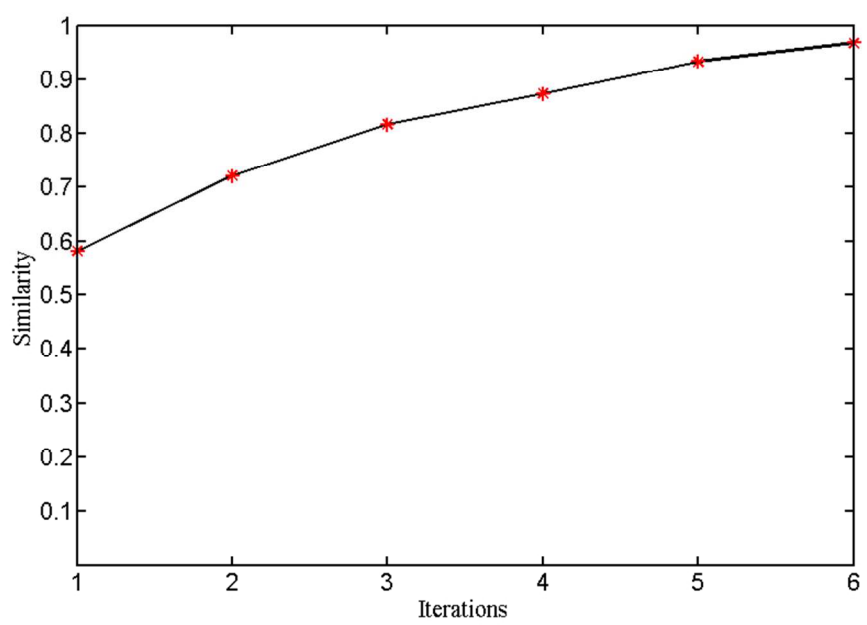
1
2
3
4
5
6
7
8
9
10
11
12
13
14
15
16
17
18
19
20
21
22
23
24
25
26
27
28
29
30
31
32
33
34
35
36
37
38
39
40
41
42
43
44
45
46
47
48
49
50
51
52
53
54
55
56
57
58
59
60



DMN statistical template mapped onto the anatomical template
85x47mm (300 x 300 DPI)

Review Only

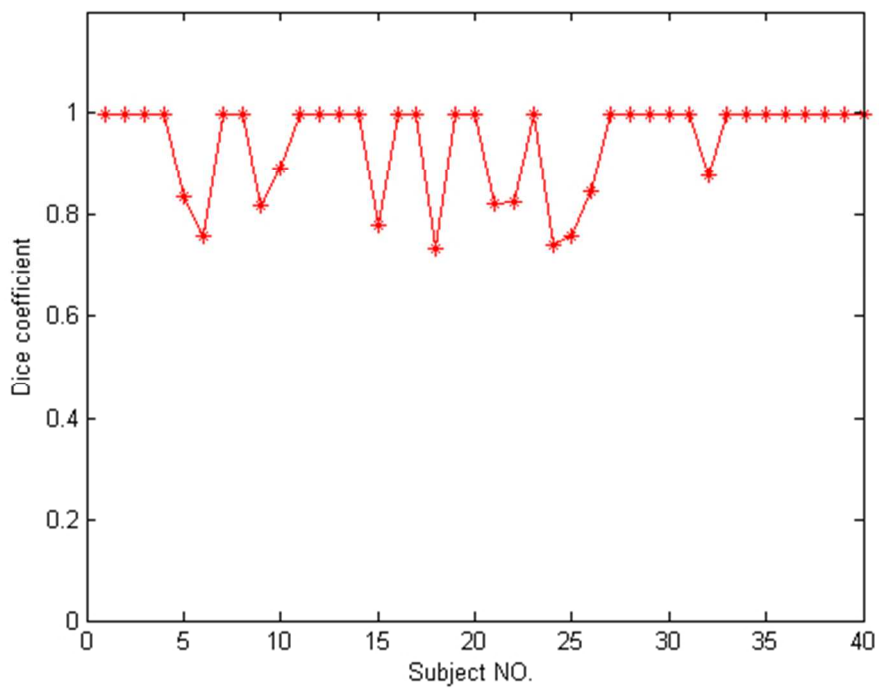
1
2
3
4
5
6
7
8
9
10
11
12
13
14
15
16
17
18
19
20
21
22
23
24
25
26
27
28
29
30
31
32
33
34
35
36
37
38
39
40
41
42
43
44
45
46
47
48
49
50
51
52
53
54
55
56
57
58
59
60



Similarities between templates of adjacent stage during the iterations
241x160mm (96 x 96 DPI)

Review Only

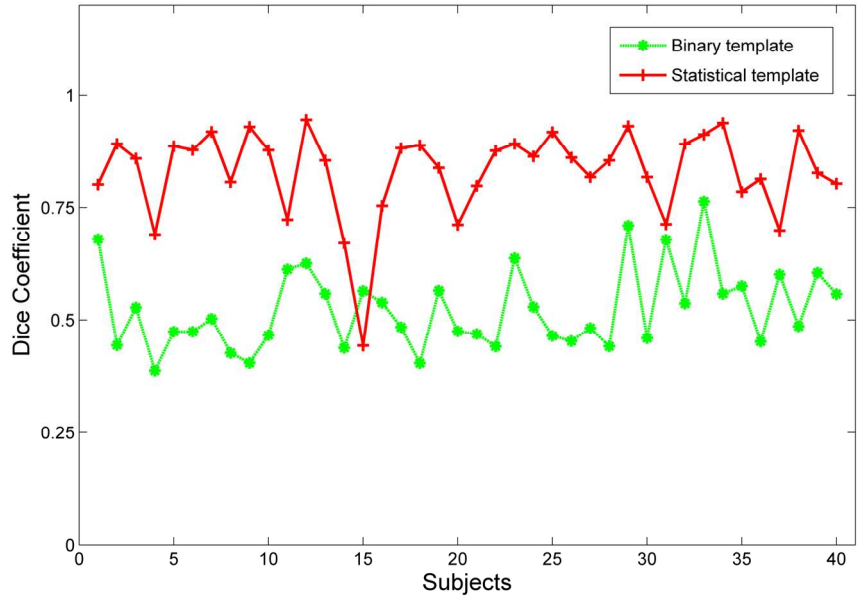
1
2
3
4
5
6
7
8
9
10
11
12
13
14
15
16
17
18
19
20
21
22
23
24
25
26
27
28
29
30
31
32
33
34
35
36
37
38
39
40
41
42
43
44
45
46
47
48
49
50
51
52
53
54
55
56
57
58
59
60



Dice coefficients between automatic and manual DMN selection
148x111mm (96 x 96 DPI)

View Only

1
2
3
4
5
6
7
8
9
10
11
12
13
14
15
16
17
18
19
20
21
22
23
24
25
26
27
28
29
30
31
32
33
34
35
36
37
38
39
40
41
42
43
44
45
46
47
48
49
50
51
52
53
54
55
56
57
58
59
60



Comparison of dice coefficients of the manually selected DMN with the statistical template and the initial binary template
160x106mm (300 x 300 DPI)

Preprint Only